Nonlinear intersubband optical absorption of asymmetric semiconductor quantum wells pumped by terahertz and infrared fields

Hai-Yan Zhu[1,2], Tong-Yi Zhang[1] and Wei Zhao[1]
[1]State Key Laboratory of Transient Optics and Photonics, Xi'an Institute of Optics and Precision Mechanics, Chinese Academy of Sciences, 17 Xinxi Road, Xi'an 710119, People's Republic of China
[2]Graduate School of the Chinese Academy of Sciences, Beijing 100039, People's Republic of China

ABSTRACT

We investigate the conduction intersubband linear response of a n-type quantum well driven by one or two infrared optical fields with arbitrary strengths. The fields couple the third subband to the second energy subband and the ground subband, forming a Λ system. We investigate the dependences of the absorption spectrum on the pump field strengths. The results for the equal Rabi frequencies can be understood in terms of quantum coherence processes of the intersubband transitions, such as coherent population trapping, and electromagnetically induced transparency. The effects of different Rabi frequencies on the absorption spectrum due to fields are also discussed.

Keywords: intersubband transition, steady state, linear absorption theory

1. INTRODUCTION

In the past few years, there has been considerable interest in the control of the linear and nonlinear optical properties of semiconductor quantum wells by use of external electric fields. The application of a static electric field can lead to the well-known Franz-Keldysh effect (FKE), i.e., pronounced oscillations occurring in the optical absorption spectrum above the band gap and nonvanishing exponential absorption tail below the band gap.[1,2] The FKE is also extended to the dynamical Franz-Keldysh effect (DFKE) in the presence of a time-dependent electric field. The DFKE predicts that the band edge should blueshifted by the ponderomotive energy, $E_{pron} = e^2F_0^2/4m\Omega^2$ (i.e., the average kinetic energy of a particle of mass m and charge e in an electric field $F_0\cos(\Omega t)$).[3,4] In the recent years, the influence of a strong terehertz field, which couples the two conduction subbands, on the interband absorption of quantum well (QW) structures was also investigated theoretically due to the obtainability of strong coherent terahertz sources.[5–11] Many interesting optical phenomena have been predicted theoretically and partly verified experimentally, such as the ac Stark effect,[12,13] harmonic generation,[14] and terahertz sideband generation.[15,16]

In this paper we investigate theoretically the probe absorption spectra of a three-subband asymmetric semiconductor QW driven by terahertz and infrared fields. The method used in the present calculation is based on a three-level density matrix theory, solving the density matrices in the steady state limit and using linear absorption theory to generate absorption spectra. The formulas describing the absorption spectra are very convenient for numerical investigations, however, they are failing to provide a transparent and readily interpretable form about the physics of the problem. In order to understand the interesting features of intersubband transitions we adopt dressed-state picture.[17,18] This picture is useful for examining the coupling mechanisms in the system and the origin of the gain and absorption. We investigate in detail the effect of varying coupling field intensity on the linear absorption of a probe field that is tunable between the three possible transitions of the considered system. The absorption spectra show one- or two-photon coupling in the system, and some distinctive quantum interference features such as coherent population trapping (CPT)[19] and electromagnetically induced transparency (EIT).[20]

Further author information:
H.Y.Z.: E-mail: haiyanvvv@opt.ac.cn
T.Y.Z.: E-mail: tyzhang@opt.ac.cn, Telephone: 86-29-88888049.

International Symposium on Photoelectronic Detection and Imaging 2009: Terahertz and High Energy Radiation Detection Technologies and Applications, edited by X.-C. Zhang, James M. Ryan, Cun-lin Zhang, Chuan-xiang Tang, Proc. of SPIE Vol. 7385, 73851Z · © 2009 SPIE · CCC code: 0277-786X/09/$18 · doi: 10.1117/12.835726

2. MICROSCOPIC THEORETICAL MODEL

We consider a n-doped three-level step asymmetric QW structure which contains three conduction subbands, exposed to two infrared optical fields polarized along the growth direction of the QW. As shown in the inset of Fig. 1(a), two laser fields with frequency ω_1 and ω_2 couple, respectively, the first, $|1>$, and second, $|2>$, levels of this system with the third level, $|3>$. In the interaction representation, and under the rotating wave approximation, the interaction Hamiltonian H_{int} is give by

$$H_{int} = \hbar\mu_{13}E_1(t)(a_3^\dagger a_1 + a_1^\dagger a_3) + \hbar\mu_{23}E_2(t)(a_3^\dagger a_2 + a_2^\dagger a_3). \tag{1}$$

Here, the first term is the interaction term of the first field, with amplitude E_1, and the second term is that of the second field, with amplitude E_2. The symbols μ_{ij} denote the magnitudes of the transition dipole matrix elements between the corresponding conduction subbands along the growth direction of the QW. $a_i^\dagger$ and a_i are electron creation and annihilation operators for an electron in the ith level, respectively.

The time evolution of this system, denoted with the density operator ρ, is governed by the master equation

$$\frac{d\rho}{dt} = -\frac{i}{\hbar}[H_{int}, \rho] + \gamma\rho, \tag{2}$$

where $\gamma\rho$ is the irreversible part that describes the effects of spontaneous emission and, possibly, other collisional relaxation processes which we treat phenomenologically. The explicit form of the equations of motion, Eq. (2), for the density matrix elements take the form:

$$\frac{d\rho_{11}}{dt} = -i\Omega_{13}\left(\rho_{31} - \rho_{13}\right) + \gamma_2\rho_{22} + \gamma_1\rho_{33}, \tag{3a}$$

$$\frac{d\rho_{22}}{dt} = -i\Omega_{23}\left(\rho_{32} - \rho_{23}\right) - \gamma_2\rho_{22} + \gamma_3\rho_{33}, \tag{3b}$$

$$\frac{d\rho_{33}}{dt} = -i\Omega_{13}\left(\rho_{13} - \rho_{31}\right) - i\Omega_{23}\left(\rho_{23} - \rho_{32}\right) - \gamma_1\rho_{33} - \gamma_3\rho_{33}, \tag{3c}$$

$$\frac{d\rho_{12}}{dt} = (i\Delta_{12} - \gamma_{12}/2)\rho_{12} + i\Omega_{23}\rho_{13} - i\Omega_{13}\rho_{23}^*, \tag{3d}$$

$$\frac{d\rho_{23}}{dt} = (i\Delta_{23} - \gamma_{23}/2)\rho_{23} - i\Omega_{23}\left(\rho_{33} - \rho_{22}\right) + i\Omega_{13}\rho_{12}^*, \tag{3e}$$

$$\frac{d\rho_{13}}{dt} = (i\Delta_{13} - \gamma_{13}/2)\rho_{13} - i\Omega_{13}\left(\rho_{33} - \rho_{11}\right) + i\Omega_{23}\rho_{12}, \tag{3f}$$

together with $\rho_{ji} = \rho_{ij}^*$. Here, $\Omega_{13} = -\mu_{13}E_1/\hbar$ and $\Omega_{23} = -\mu_{23}E_2/\hbar$ are the Rabi frequencies of the coupling laser field and the corresponding transition. Δ_{23} and Δ_{13} denote the one-photon detunings and $\Delta_{12} = \Delta_{13} - \Delta_{23}$ the two-photon detuning of the coupling laser frequency from the electronic resonances. The population scattering rates γ_i are due primarily to longitudinal optical phonon emission events at low temperature. The total dephasing rates $\gamma_{ij}(i \neq j)$ are given by $\gamma_{12} = (\gamma_2 + \gamma_{12}^{dph}), \gamma_{23} = (\gamma_1 + \gamma_2 + \gamma_3 + \gamma_{23}^{dph})$, and $\gamma_{13} = (\gamma_2 + \gamma_{12}^{dph})$, where the pure dipole dephasing rates γ_{ij}^{dph} are assumed to be due to a combination of quasielastic interface roughness scattering or acoustic phonon scattering. A comprehensive treatment of the decay rates would involve incorporation of the decay mechanisms into the Hamiltonian of the system. However, we have adopted the phenomenological approach of treating the decay mechanisms. In addition, we have taken the three subbands to have the same effective mass. So the kth dependence of the above parameters has been suppressed, where k is the in-plane wave vector.

To study the linear absorption response of the system discussed above we adopt the procedure of Manka et al..[21] The absorption coefficient of a weak probe field, which has the same polarization as those of the pump fields but with tunable frequency, is given by

$$\alpha(\omega_p) = \alpha_{12}(\omega_p) + \alpha_{23}(\omega_p) + \alpha_{13}(\omega_p), \tag{4}$$

where

$$\alpha_{12}(\omega_p) = \mathrm{Re}\, F < [p_{12}^{+}(\tau), p_{12}^{-}(0)] >, \tag{5}$$

$$\alpha_{23}(\omega_p) = \mathrm{Re}\, F < [p_{23}^{+}(\tau), p_{23}^{-}(0)] >, \tag{6}$$

and

$$\alpha_{13}(\omega_p) = \mathrm{Re}\, F < [p_{13}^{+}(\tau), p_{13}^{-}(0)] > \tag{7}$$

are the absorption coefficients for the corresponding three possible transitions. Here, ω_p is the probe frequency, the symbol F denote the Fourier transform operation, and

$$\begin{aligned} p_{12}^{+} &= \mu_{12} a_1^{\dagger} a_2, \\ p_{23}^{+} &= \mu_{23} a_2^{\dagger} a_3, \\ p_{13}^{+} &= \mu_{13} a_1^{\dagger} a_3, \end{aligned} \tag{8}$$

and p_{ij}^{-}, which is given by the complex conjugate of p_{ij}^{+}, are the positive and negative parts of the dipole polarization operator for the three-level QW system.

With the help of the quantum regression theorem,[22] we derive the expressions for Eqs. (5)-(7) to calculate the two-time expectation values under steady-state conditions. The motion equations are integrated twice: once to yield the steady state density matrix elements and secondly to yield the two-time expectation values.

3. NUMERICAL RESULTS AND DISCUSSION

As a model material system, we consider a GaAs/AlGaAs QW system. The core of the structure consists of three layers: a 3.8 nm GaAs layer followed by 24.2 nm $Al_{0.25}Ga_{0.75}As$, confined by 20 nm $Al_{0.39}Ga_{0.61}As$ barriers on both sides. The barrier height (relative to the deep well) is 300 meV and the step barrier height is 100 meV. The band edge separations are: $E_3 - E_2 = 17$ and $E_3 - E_1 = 126$ meV. The electron density of the QW is such sheet that the electron-electron effects have little influence in our results. Therefore, the effects of electron-electron interactions are not included in our study. An infrared field with frequency ω_1 and a THz laser field with frequency ω_2 are assumed to be coupled individually to the resonances $1 \rightarrow 3$ (ω_{13}) and $2 \rightarrow 3$ (ω_{23}). In our numerical calculations, the total collision rates are set to be $\Gamma_1 = \Gamma_2 = \Gamma_3 = 0.6$ ps, $\Gamma_{21} = 1.0$ ps, $\Gamma_{31} = 1.2$ ps, and $\Gamma_{32} = 1.5$ ps, respectively.

Figure 1 shows the dependence of the absorption spectra corresponding to the three possible transitions on the equal Rabi frequency ($\Omega_{23} = \Omega_{13} \equiv \Omega$) under the resonant transitions. The line shape due to the $1 \rightarrow 2$ transition varying with the Rabi frequency Ω is shown in Fig. 1(a). In the presence of very weak fields ($\Omega = 0.5$ meV) we see that the $1 \rightarrow 2$ transition spectrum is a standard Lorentzian line. When Ω increases to 4 meV, however, the absorption is strongly suppressed. For $\Omega = 8$ and 12 meV the absorption virtually vanishes. This strong suppression occuring is because most of the electron population is equally distributed between the first and second levels due to CPT (see Fig. 2(b)). Fig. 1(b) shows the absorption spectrum due to the $2 \rightarrow 3$ transition. When the pump field is very weak ($\Omega = 0.5$ meV) the $2 \rightarrow 3$ transition spectrum shows an obviously gain at the resonant frequency. Here, the probe field intensity is comparable with the weaker pump field so as to influence electron population of the steaded-state system. The electron population of the steaded-state system for all three levels are obtained by integrating Eq. (2), the results being shown in Fig. 2. For a weaker pump field, say $\Omega = 0.5$ meV, [Fig. 2(a)], electron population experiences no obvious Rabi oscillations and are larger in the second level than in the third level when the system becomes steady. Thus the appearance of the gain peak does not rely on the population inversion. For higher field intensities, the gain peak becomes suppressed in amplitude drastically and fades out gradually while double-peaked absorption spectrum starts to appear. The

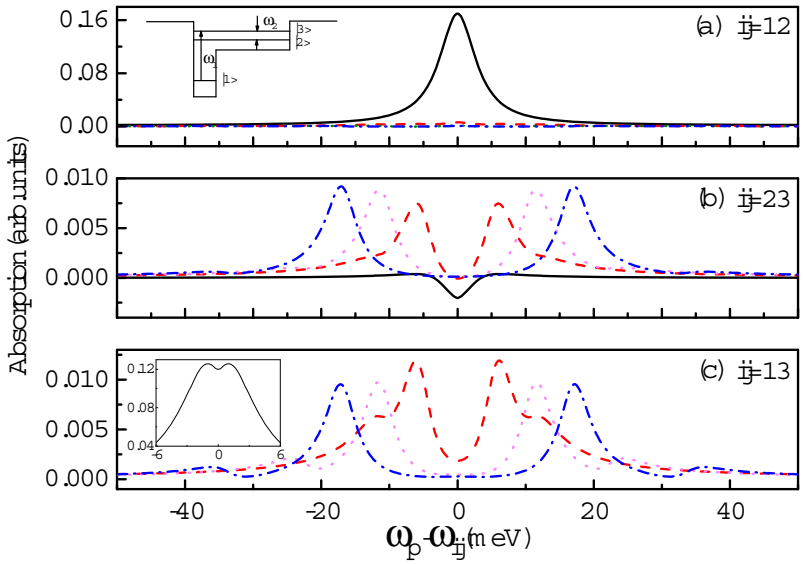

Figure 1. (Color online) Linear absorption response of an asymmetric quantum well under the resonant coupling field configuration, i.e., $\omega_1 = \omega_{31}$ and $\omega_2 = \omega_{32}$. Parts (a), (b) and (c) show, respectively, the contribution due to the $1 \rightarrow 2$, $2 \rightarrow 3$, $1 \rightarrow 3$ transitions. The Rabi frequencies corresponding to each line are solid: $\Omega = 0.5$ meV; dashed: $\Omega = 4.0$ meV; dotted: $\Omega = 8.0$ meV; dash-dotted: $\Omega = 12$ meV. The inset of (a) denotes the schematic of the energy level arrangement for the asymmetric quantum wells. Subband levels are labeled in ascending energy: |1>, |2>, and |3>. There are three possible optical transitions (frequencies): $1 \rightarrow 2$ (ω_{21}),$1 \rightarrow 3$ (ω_{31}), $2 \rightarrow 3$ (ω_{32}). Two coupling field with optical frequencies ω_1 and ω_2 couple separately to the transitions $1 \rightarrow 3$ and $2 \rightarrow 3$, respectively.

two peaks become larger and move away from the central frequency as the pump intensity is increased. Figure 1(c) indicates the absorption spectrum associated with the $1 \rightarrow 3$ transition. When the pump field intensities become higher, two symmetric pairs of sidebands spaced by $\pm\sqrt{2}\Omega$ and $\pm 2\sqrt{2}\Omega$ from the center appear in the absorption spectrum.

In order to understand the origin of the spectra features at higher field intensity in Fig. 1(b) and (c) we adopt the dressed-state picture. This set of states can be constructed as follows for a general Λ model, in which the two field intensities can be different:

$$|r>_\Lambda = -\sin\theta|1> + \cos\theta|2>, \tag{9}$$

$$|s>_\Lambda = \frac{1}{\sqrt{2}}[\cos\theta|1> + \sin\theta|2> + |3>], \tag{10}$$

$$|t>_\Lambda = \frac{1}{\sqrt{2}}[\cos\theta|1> + \sin\theta|2> - |3>]. \tag{11}$$

Here $|s>_\Lambda$and $|t>_\Lambda$are one-photon dressed states which are the results of mixing of all three levels and the angle θ is connected to the ratio of the two Rabi frequencies according to the equation

$$\tan\theta = \frac{\Omega_{23}}{\Omega_{13}}. \tag{12}$$

Since these states are eigenstates of H_{int}, we have

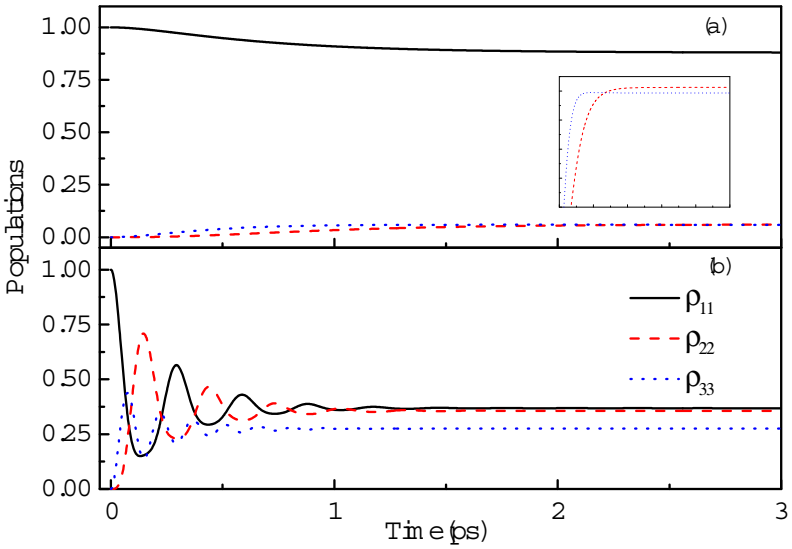

Figure 2. (Color online)Time evolution of the quantum well electron populations for all three levels $|1>$(solid line), $|2>$(dashed line), $|3>$(dotted line) under the two resonant coupling fields. (a) $\Omega_{13} = \Omega_{23} = 0.5$ meV; (b) $\Omega_{13} = \Omega_{23} = 10$ meV. The inset of (a) is the enlarged parts of the two upper levels to show the steady-state population clearly.

$$H_{int}|s>_\Lambda = \hbar\Omega^{'}|s>_\Lambda, \tag{13}$$

$$H_{int}|t>_\Lambda = -\hbar\Omega^{'}|t>_\Lambda, \tag{14}$$

where $\Omega^{'} = \sqrt{\Omega_{23}^2 + \Omega_{13}^2}$. On the other hand, the two-photon state $|r>_\Lambda$, which is the result of a two-photon dressing process between QW-field states associated with $|1>$ and $|2>$, has the same energies as the corresponding bare states, i.e.,

$$H_{int}|r>_\Lambda = 0. \tag{15}$$

Consider the double-peaked spectra shown in Fig. 1(b). Under resonant coupling, the one-photon states have less population than the two-photon state.[23] The double peaks here is the result of transitions between the two-photon state in the second level $|2, r>$ and the one-photon states in the third level $|3, s>$ and $|3, t>$. The energy separations between them are $\omega_2 - \sqrt{2}\Omega$ and $\omega_2 + \sqrt{2}\Omega$, respectively. The amplitude increasing of the double peaks ascribes to the augmenting of the population difference between 2 and 3 levels, i.e., $n_2 - n_3$. According to the intersubband transition rate equation,[24, 25] the intersubband pump rate is proportional to the pump field strength. When the pump field strength is enhanced, more electrons in the third level would be pumped to the second level, which can also be seen from Fig. 2(b). Thus, for higher field intensities, the absorption peaks would be increased gradually with the increasing of the pump fields intensity. The sidebands spaced by $\pm\sqrt{2}\Omega$ from the center in Fig. 1(c) result from, similar to the two absorption peaks associated with the $2 \rightarrow 3$ transition, the transitions between the two-photon state in the first level $|1, r>$, and two one-photon states in third level, $|3, s>$ and $|3, t>$. Their corresponding frequencies are at $\omega_1 - \sqrt{2}\Omega$ and $\omega_1 + \sqrt{2}\Omega$, respectively. The story is rather different for another symmetric pairs of sidebands in the absorption spectrum. Here the absorption of the infrared field is accompanied by transitions between two one-photon states. For the photon absorbed with

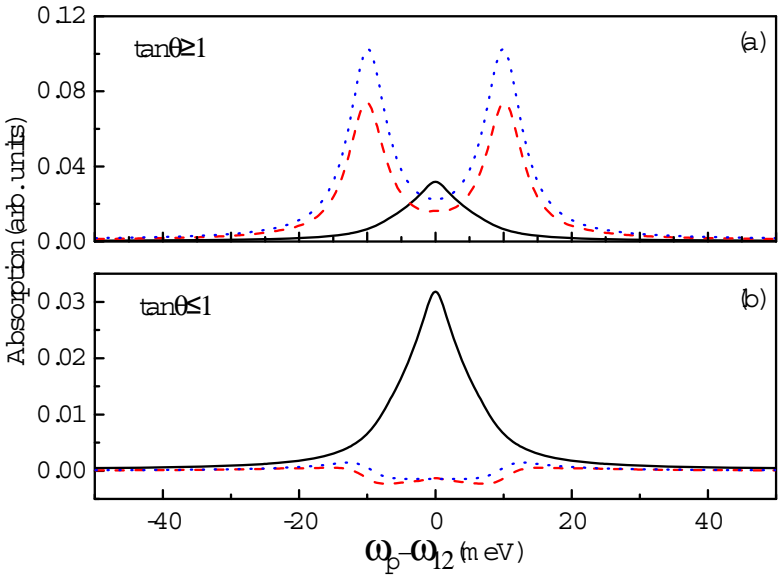

Figure 3. (Color online) The contribution of the $1 \rightarrow 2$ transition to the linear absorption of a weak probe field. In both parts, the solid line corresponds to $\Omega_{13} = \Omega_{23} = 2$ meV. In (a) the dashed line is for $\Omega_{13} = 2$ meV and $\Omega_{23} = 10$ meV, and the dotted line is for $\Omega_{13} = 0$ and $\Omega_{23} = 10$ meV. In (b) the dashed line is for $\Omega_{13} = 10$ meV and $\Omega_{23} = 2$ meV, and the dotted line is for $\Omega_{13} = 10$ and $\Omega_{23} = 2$ meV.

frequency $\omega_1 - 2\sqrt{2}\Omega$ these states are $|1, s>$ and $|3, t>$, while for the photon with frequency $\omega_1 + 2\sqrt{2}\Omega$ they are $|1, t>$ and $|3, s>$.

In the above, the effects of the Rabi frequency with $\Omega_{23} = \Omega_{13}$ on the probe absorption spectrum have been discussed. To further the analysis of the nonlinear effects caused by quantum interference, we now see what happens to the absorption under the resonant transitions if $\Omega_{23} \neq \Omega_{13}$. Figure 3 shows that the linear absorption spectrum due to the $1 \rightarrow 2$ transition varies as the Rabi frequencies of the coupling fields. As a comparison with the spectrum of the equal Rabi frequencies, the linear response for $\Omega_{23} = \Omega_{13} = 2$ meV is also plotted in Fig. 3 (solid line). When Ω_{23} is increased by five times while Ω_{13} remains unchanged, the absorption spectrum becomes a doublet (dashed line). For the case of $\Omega_{23} = 10$ meV and $\Omega_{13} = 0$, the amplitude of the doublet is increased evidently (dotted line). These changes origins from field-coherence destruction. As Eqs. (9)-(11) indicate, the unequal Rabi frequecies of the coupling fields cause one state to be decoupled from the rest of the system. The stronger field can destroy the coherences generated by the weaker field. The increasing amplitude for the case $\Omega_{23} = 10$ and $\Omega_{13} = 2$ meV implies that increasing Ω_{23} decreases the effect of the weaker infrared field, which suppress the excitation of electrons in the ground level. Further increasing of the absorption peak for the case $\Omega_{23} = 10$ meV and $\Omega_{13} = 0$ comes from the fact that the absence of the infrared field make more electrons stay in the ground level. The double peaks in Fig. 3(a) denotes the electromagnetically induced transparency owing to quantum inteferences. Fig. 3(b) shows the inverse case for the same absorption spectrum associated with $1 \rightarrow 2$ transition, i.e., $\tan\theta \leq 1$. Here the solid line still corresponds to $\Omega_{23} = \Omega_{13} = 2$ meV. When Ω_{13} is increased by five times, the absorption spectrum display extensive gain at the resonant frequency (dashed line). The line shape of the spectrum for $\Omega_{23} = 0$ and $\Omega_{13} = 10$ meV is identical with the dashed line in addition to the trifling numerical differences (dotted line). In both cases, the gain is because more electrons in the ground level are pumped to the third level by the infrared field, and then are excited or fast decay into the second level through LO-phonon emission.

4. CONCLUSIONS

In conclusion, we have presented a detailed investigation of the nonlinear optical absorption of intersubband transitions in an asymmetric n-doped QW structure driven by two laser fields. The dependences of absorption spectra on the intensity of the two pump fields are analyzed by a dressed-state picture. The results show quantum coherent effects such as electromagneticlly induced transparency in presence of two equal Rabi frequency, and reveal how coherence destruction could occur when the Rabi frequencies due to the fields become different.

ACKNOWLEDGMENTS

This work is Supported by the National Basic Research Program of China (973 Program)(2007CB310405), the National Natural Science Foundation of China (Grant No. 60777017 and 10834015), K. C. Wong Education Foundation, Hong Kong.

REFERENCES

1. L. V. Keldysh, Zh. Eksp. Teor. Fiz. **34**, 1118 1958 [Sov. Phys. JETP **7**, 788 (1958)].
2. T. Y. Zhang, W. Zhao, X. M. Liu, and C. Zhang, Appl. Phys. Lett. **91**, 041909 (2007).
3. Y. Yacoby, Phys. Rev. **169**, 610 (1968).
4. A. Srivastava, R. Srivastava, J. Wang, and J. Kono, Phys. Rev. Lett. **93**, 157401 (2004).
5. Tong-Yi Zhang and Wei Zhao, Europhys. Lett., **82**, 67001 (2008).
6. J. Kono *et al.*, Phys. Rev. Lett. **79**, 1758 (1997).
7. V. Ciulin, S. G. Carter, and M. S. Sherwin, Phys. Rev. B **70**, 115312 (2004).
8. S. G. Carter *et al.*, Phys. Rev. B **72**, 155309 (2005).
9. B.J. Keay *et.al.*, Phys. Rev. Lett. **75,** 4098 (1995).
10. J. C. Cao, Phys. Rev. Lett. **91,** 237401 (2003).
11. A. G. Markelz, N. G. Asmar, B. Brar, and E. G. Gwinn, Appl. Phys. Lett. **69,** 3975 (1996).
12. J. F. Dynes *et al.*, Phys. Rev. L **94**, 157403 (2005).
13. A. V. Maslov and D. S. Citrin, Phys. Rev. B **64**, 155309 (2001).
14. J. N. Heyman *et at.*, Phys. Rev. Lett. **72**, 2183 (1994).
15. Hai-Yan Zhu, Tong-Yi Zhang, and Wei Zhao, J. Appl. Phys. **105**, 043518 (2009).
16. P. Aceituno, A Hernández-Cabrera, and F T Vasko, J. Phys.:Condens. Matter **17**, 6925 (2005).
17. C. Cohen-Tannoudji and S. Reynaud, J. Phys. B: Atom. Molec. Phys., **10**, 345 (1977).
18. T. A. B. Kennedy, and S. Swain, Phys. Rev. A **36,** 1747 (1987).
19. E. Arimondo, Phys. Rev. A **54**, 2216 (1996).
20. G. B. Serapiglia et al., Phys.Rev. Lett. **84**, 1019 (2000).
21. A. S. Manka, E. J. D′Angelo, L. M. Narducci, and M. O. Scully, Phys. Rev. A **47**, 4236 (1993).
22. L. M. Narducci *et al.*, Phys. Rev. A **42**, 1630 (1990).
23. S. M. Sadeghi, S. R. Leffler, and J. Meyer, Phys. Rev. B **59**, 15388 (1999).
24. R. Palella, *Intersubband Transitions in Quantum Structures* (McGraw-Hill, 2006).
25. A. Liu and C. Z. Ning, Appl. Phys. Lett. **75**, 1207 (1999).